# Electronic Energy States of Dislocations in CdS-Type Semiconductors*

R. R. HOLMES† AND C. ELBAUM
*Department of Physics, Brown University, Providence, Rhode Island 02912*
(Received 13 May 1968)

It is shown that electronic energy bands are associated with dislocations in wide-band-gap, compound semiconductors. The eigenvalue problem for the dislocation band edge is solved for CdS-type crystals, and the occupation of the band is calculated. The Fermi energy is then determined for crystals containing many deep-lying discrete levels as well as dislocation bands. It is predicted that when a crystal is illuminated with light of appropriate wavelength and increasing intensity, the thermal activation energy governing the electrical conductivity passes through a series of energy plateaus which are equal to the energy of the discrete levels. In a dislocation-free crystal, these plateaus are connected by step changes, while in a crystal with dislocations they are connected by broad transition regions. In order to study the predictions, the thermal activation energy was measured as a function of light intensity in both deformed and undeformed samples of CdS. In all cases, plateaus at $0.80\pm0.02$ and $0.06\pm0.02$ were observed. The transition between these plateaus was sharp in the case of the undeformed samples and broad in the case of the deformed samples. These results confirm the predictions mentioned above.

## 1. INTRODUCTION

NEAR a dislocation, changes in the energy of an electron in a crystal may arise from lattice dilatation and in the case of edge dislocations from unpaired bonds.[1] Heine[2] shows that lattice dilatation can lead to a discrete energy level in the forbidden gap. Emtage,[3] who has treated this problem in greater detail, concludes that this effect is overwhelmed by the dangling bonds, and lattice dilatation is relevant only in the case of screw dislocations.

Two important properties arise from the geometric proximity of the unpaired or "dangling" bonds. First, the wave function for adjacent sites should overlap significantly, which suggests a band of energy levels. Second, the occupation of an energy level associated with the dislocation edge should be limited by the Coulomb energy associated with the trapped charge carriers.

In a treatment of these states, Read[4–6] assumed that the overlap of the wave function was unimportant, and he concentrated on the electrostatic energy. He postulated that the dangling bonds lead to acceptor states at a discrete energy, and that their occupation is severely limited by the mutual Coulomb repulsion of the trapped electrons.

On the other hand, Bonch-Bruevich and Glasko[7] solve the problem in terms of a quantum-mechanical model in which a trapped hole is free to move along the dislocation edge, and the electrostatic energy is a small perturbation. They predict energy bands in which the band edge is determined by the bound two-dimensional motion of the trapped hole in the plane normal to the dislocation edge, and the bandwidth arises from the unconstrained motion of the trapped hole along the dislocation edge.

Because both of these theories have adjustable parameters, it has not been possible to distinguish between them experimentally. For example, Logan *et al.*[8] obtained results on deformed Ge which they explained in terms of Read's theory. Later, Gulyaev[9] was able to reinterpret these results in terms of a band model. One of the reasons for the ambiguity is the choice of material—Ge. Gulyaev finds that the dislocation band in Ge falls below the Fermi level, with the result that the temperature dependence of the dislocation occupation is similar to that of a discrete level. In addition, since Ge forms covalent bonds, the binding energy of a hole to a dislocation is a strong function of dislocation occupation. Gulyaev[9] finds that this leads to an unspecified shift in the band edge with occupation.

CdS has advantages over Ge for the study of dislocation energy bands. These include the following:

(1) In CdS, the dangling bonds are partially ionic rather than entirely covalent. Therefore, the dislocation energy states are affected less by the charge on the dislocation than they are in Ge.

(2) In CdS we often find a high density of deep levels which are associated with various impurities and other point defects. As we will show later these energy levels, which will be referred to as *local levels* can be used as a probe of the dislocation band.

In the present work, the band theory for dislocation energy states is formulated for CdS, and the resulting eigenvalue equation is solved for the dislocation band edge by using a pseudo-square-well approximation for the dislocation potential. The dislocation occupation is then calculated as a function of the Fermi

* Research supported in part by the Office of Naval Research.
† National Science Foundation Coop. Fellow 1964–1966. Present address: Bell Telephone Laboratories, Whippany, N. J.
[1] W. Shockley, Phys. Rev. **91**, 228 (1953).
[2] V. Heine, Phys. Rev. **146**, 568 (1966).
[3] P. R. Emtage, Phys. Rev. **163**, 865 (1967).
[4] W. T. Read, Phil. Mag. **45**, 775 (1954).
[5] W. T. Read, Phil. Mag. **45**, 1119 (1954).
[6] W. T. Read, Phil. Mag. **46**, 111 (1955).
[7] V. L. Bonch-Bruevich and V. B. Glasko, Fiz. Tverd. Tela **3**, 36 (1961) [English transl.: Soviet Phys.—Solid State **3**, 26 (1961)].
[8] R. A. Logan, G. L. Pearson, and D. A. Kleinman, J. Appl. Phys. **30**, 885 (1959).
[9] Yu. V. Gulyaev, Fiz. Tverd. Tela **3**, 1094 (1961) [English transl.: Soviet Phys.—Solid State **3**, 796 (1961)].

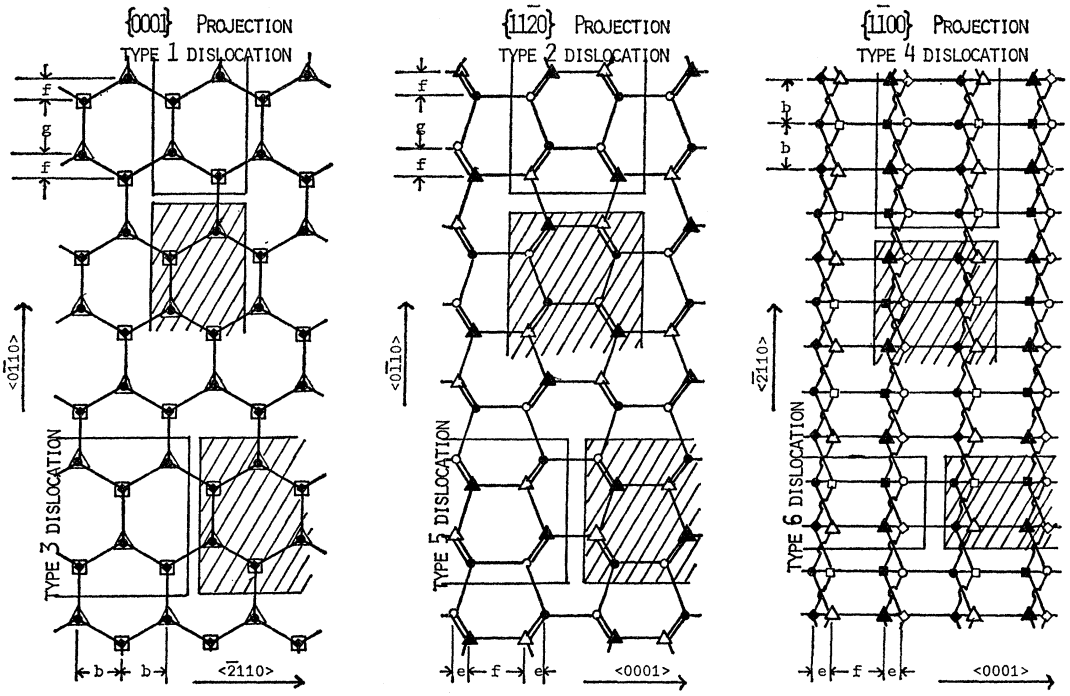


FIG. 1. Geometric projections of atomic planes in CdS. For key and explanations see the text.

energy, and this result is combined with a general description of a wide-band-gap semiconductor containing many deep levels. This derivation leads to the prediction that in CdS with a low dislocation density the activation energy associated with the temperature dependence of the electrical conductivity will coincide with a local level, whereas in CdS with a high dislocation density the activation energy may fall between two such levels. This prediction has been verified in experiments with undeformed and deformed CdS crystals.

## 2. DISLOCATION GEOMETRY IN HEXAGONAL CdS

Figure 1 shows the geometric projection of various planes of atoms from three directions of high symmetry. Each projection represents several superposed planes, and atoms on different planes are designated by triangles, circles, squares, and diamonds. Solid symbols represent Cd atoms, and unshaded symbols represent S atoms. In the {0001} projection, the atoms from two of the projected planes lie directly behind atoms from two other planes. This is indicated by a double symbol. The dimensions indicated have the following values: $b=2.07$ Å; $d=2.52$ Å; $e=0.84$ Å; $f=1.19$ Å; $g=2.39$ Å.

Because the ⟨0001⟩, ⟨1$\bar{1}$00⟩, and ⟨11$\bar{2}$0⟩ directions can be mutually perpendicular, it is possible to construct edge dislocations with their Burgers vector in one of these directions, and their edge in another. There are six such systems. In each of the projections of Fig. 1, solid lines enclose the extra half-planes of the two dislocations whose Burgers vectors lie in the plane of the projection. The shaded areas represent atoms that would be missing if the dislocation terminated as indicated. Many of the geometric properties of these six dislocation systems are summarized by Table I.

In the present experiment it is postulated that type-6 dislocations are introduced for the following reasons. First, the applied (longitudinal) stress formed an angle of 45° with both the ⟨0001⟩ and the ⟨11$\bar{2}$0⟩ directions. As may be deduced from Table I, this maximizes the probability for the generation of the type-6 dislocations. Second, our deformation occurred at temperatures below 580°C, and in bending experiments, Shiozawa and Jost[10] found that only slip involving the type-6 dislocations occurred in this temperature range.

Two important properties of the type-6 dislocation should be indicated. First, as shown in Table I, these dislocations terminate either in all Cd atoms, or in all S atoms and therefore are either acceptor or donor type. Figure 1 shows that the type of atom which terminates the dislocation does not change with jogs or steps. Whether the type-6 dislocation is acceptor or donor type is completely determined by the sense of the Burgers vector. Second, the edge of the type-6 dislocation is a line of broken, partially ionic bonds which zig-zag between the extra two half-planes. It is assumed that there is significant overlap of the potential of adjacent broken bonds, and the potential associated

[10] L. R. Shiozawa and J. M. Jost, Aerospace Research Laboratories Report No. ARL-65-98, 1965 (unpublished).

TABLE I. Properties of principal types of dislocations in CdS.

| Dislocation type | Burgers vector | Slip plane | Dislocation edge | Type and number of extra half-planes | Description of the edge |
|---|---|---|---|---|---|
| 1 | $\langle 11\bar{2}0\rangle$ | $\{1\bar{1}00\}$ | $\langle 0001\rangle$ | Mixed (2)[a] | One line of alternating Cd and S atoms, each atom having one broken bond. |
| 2 | $\langle 0001\rangle$ | $\{1\bar{1}00\}$ | $\langle 11\bar{2}0\rangle$ | All Cd (2)<br>All S (2) | Two lines of atoms; one of all Cd atoms, and one of all S atoms. Each atom has one broken bond. |
| 3 | $\langle 1\bar{1}00\rangle$ | $\{11\bar{2}0\}$ | $\langle 0001\rangle$ | Mixed (4) | Two lines of alternating Cd and S atoms. Each atom has one broken bond. |
| 4 | $\langle 0001\rangle$ | $\{11\bar{2}0\}$ | $\langle 1\bar{1}00\rangle$ | All Cd (2)<br>All S (2) | Four lines of atoms; two of all Cd atoms, and two of all S atoms. Each atom has one broken bond. |
| 5 | $\langle 1\bar{1}00\rangle$ | $\{0001\}$ | $\langle 11\bar{2}0\rangle$ | Mixed (4) | Two lines of atoms; both lines are all Cd atoms, *or* both lines are all S atoms. Each atom has one broken bond. |
| 6 | $\langle 11\bar{2}0\rangle$ | $\{0001\}$ | $\langle 1\bar{1}00\rangle$ | Mixed (2) | Two lines of atoms; both lines are all Cd atoms, *or* both lines are all S atoms. Each atom has one broken bond. |

[a] A mixed extra half-plane is a plane containing both Cd and S atoms.

with the edge looks like a tube of rectangular cross section. This feature will be used later in connection with the quantum-mechanical calculation.

## 3. DISLOCATION BANDS

Several theories for the electronic states of edge dislocations have predicted bands.[1,7,11,12] The approach which forms the basis for much of this paper was proposed by Bonch-Bruevich and Glasko.[7] Their theory is formulated in terms of holes contained in acceptor-type dislocation bands which are located below the Fermi energy.

The present derivation is formulated in terms of the electron occupation of donor bands. With simple changes of notation, these results apply to the hole occupation of acceptor bands. In this treatment the charge on the dislocation is accounted for in two ways. First, an explicit correction $V_q$ is made to the final derived energy levels. This correction is due to the fact that the total Coulomb energy of all captured holes is reduced when an electron is captured. $V_q$ is essentially the electrostatic energy $E_s$ defined by Read,[4] and it is approximately proportional to the charge on the dislocation. This means that in a type-6 dislocation $V_q$ is related to the dislocation occupation ($n_D$) by

$$V_q=-C(n_D-\tfrac{1}{2}n_s), \tag{1}$$

where $n_s$ is the number of atomic sites per unit length of dislocation and $C$ is a positive constant. The second effect of the charge on the dislocation occupation arises because the perturbing potential $V(\mathbf{r})$, associated with the dislocation, is charge-dependent. This means that the wave equation involving $V(\mathbf{r})$ must be solved in a self-consistent manner. However, in CdS the dangling bonds are partially ionic, and $V(\mathbf{r})$ does not depend strongly on dislocation occupation. We will assume that $V(\mathbf{r})$ can be specified, and that the resulting energy levels are independent of dislocation occupation.

If the energy of an electron in the conduction band is related to its momentum through $E(\mathbf{p})$, then in the effective mass approximation the "effective" Hamiltonian for the electron is $E(-ih\nabla)$. When this electron is also in the field of a dislocation, the effective wave equation is

$$[E(-ih\nabla)+V(\mathbf{r})]\Psi(\mathbf{r})=W\Psi(\mathbf{r}). \tag{2}$$

The eigenvalue $W$ represents the change of the energy of the entire crystal due to the interaction of a single electron with a dislocation.

Following Bonch-Bruevich and Glasko,[7] an approximate form of Eq. (2) is obtained by expanding the function $E(\mathbf{p})$ to quadratic terms about $(0,0,p_z)$. It is assumed that $E(\mathbf{p})$ has an extremum along this line so the first derivatives in $p_x$ and $p_y$ vanish. By choosing a coordinate system in which $z$ is along the dislocation edge, and the $x$-$y$ submatrix of the effective-mass tensor is diagonal, the expansion of $E(\mathbf{p})$ becomes

$$E(p_x,p_y,p_z)=E(0,0,p_z)+\frac{1}{2m_{xx}}p_x^2+\frac{1}{2m_{yy}}p_y^2. \tag{3}$$

If the dislocation does not disturb the periodicity of the crystal field along the dislocation edge ($z$ direction), the wave function and dislocation potential can be written as

$$\Psi(\mathbf{r})=P(x,y)e^{-ikz}, \qquad V(\mathbf{r})=V(x,y). \tag{4}$$

Combining Eqs. (2), (3), and (4) and simplifying yields

$$\left[-\frac{\hbar^2}{2m_{xx}}\frac{d^2}{dx^2}-\frac{\hbar^2}{2m_{yy}}\frac{d^2}{dy^2}+V(x,y)\right]P(x,y)=\lambda P(x,y), \tag{5}$$

[11] W. Guth and W. Haist, Phys. Status Solidi 17, 691 (1966).
[12] A. L. Laskar and C. L. Roy, Proc. Natl. Inst. Sci. India A29, 430 (1963).

where $\lambda$ is defined by

$$\lambda \equiv W - E(0,0,\hbar k). \tag{6}$$

Equations (5) and (6) can be interpreted in terms of multiple energy bands. To see this we define the zero of energy at the conduction-band edge. The function $E(0,0,\hbar k)$ then represents the kinetic energy of an electron, in the conduction band, moving in the $z$ direction with momentum $\hbar k$. Since this energy has a quasicontinuum of positive allowed values, the total energy $W$ can have a quasicontinuum of values above a band edge at $\lambda$. For any negative value of $\lambda$ these energy states constitute a band of allowed states which overlap the forbidden gap. If $\lambda$ is positive, these states represent the scattering of free electrons by the dislocation.

In order to obtain an approximate solution to Eq. (5) for the eigenvalues $\lambda$, it is assumed that, as mentioned earlier, $V(x,y)$ has the form of a rectangular "square well." (This is a crude approximation to the actual potential and its use with the effective-mass approximation is not expected to yield very rigorous results, but it should be helpful in estimating the number of bands which will be bound.) Within the well the potential is $-|V|$, and outside it is zero. The diagram of the type-6 dislocation (Fig. 1) shows that the potential of the broken bonds may extend over about three times the separation of the $\{11\bar{2}0\}$ planes in one direction, and over most of the length of the hexagonal cell in the other. Thus 6 by 8 Å is a reasonable estimate for the size of the well.

To render Eq. (5) separable, a further approximation must be made. Here the "square well" is replaced by the following potential:

$$\begin{aligned} &V(x,y)=U(x/\alpha)+U(y/\beta),\\ &U(w)=\tfrac{1}{2}|V|, \quad |w|>1\\ &U(w)=\tfrac{1}{2}|V|, \quad |w|<1 \end{aligned} \tag{7}$$

where $\alpha$ and $\beta$ are the half-widths of the well in the $x$ and $y$ directions. This potential can be compared to two intersecting streets at a level $V=0$ which run between buildings of height $V=|V|$. At the intersection of these streets there is a hole of depth $V=-|V|$. Using this potential, Eq. (5) can be written in separated form:

$$\left[-\frac{\hbar^2}{2m_{xx}}\frac{d^2}{dx^2}+U\left(\frac{x}{\alpha}\right)-(\lambda-b)\right]X(x)=0, \tag{8a}$$

$$\left[-\frac{\hbar^2}{2m_{yy}}\frac{d^2}{dy^2}+U\left(\frac{y}{\beta}\right)-b\right]Y(y)=0, \tag{8b}$$

where $b$ is a separation parameter which is real. Let

$$\begin{aligned} &u=x/\alpha, \quad E_u=\lambda-b, \quad \gamma_u{}^2=\hbar^2/2m_{xx}\alpha^2;\\ &v=y/\beta, \quad E_v=b, \quad\quad \gamma_v{}^2=\hbar^2/2m_{yy}\beta^2. \end{aligned} \tag{9}$$

When these definitions are substituted into (8a) and (8b), these two equations become dimensionless and formally identical. By letting $X(x)$ and $Y(y)\rightarrow H(w)$, $E_u$ and $E_v\rightarrow E$, $\gamma_u$ and $\gamma_v\rightarrow\gamma$ in Eqs. (8), they can be written in the regions $|w|<1$ and $|w|>1$ as follows:

$$\begin{aligned} &\frac{d^2H(w)}{dw^2}=s^2H(w), \quad |w|>1\\ &\frac{d^2H(w)}{dw^2}=-t^2H(w), \quad |w|<1 \end{aligned} \tag{10}$$

where $s$ and $t$ are defined as follows:

$$s=(1/\gamma)[\tfrac{1}{2}|V|-E]^{1/2}, \quad t=(1/\gamma)[\tfrac{1}{2}|V|+E]^{1/2}. \tag{11}$$

Since $V$ and $E$ are real, $s$ and $t$ cannot be complex, but they may be entirely imaginary or entirely real. They are by definition positive.

For Eqs. (10) to have bound solutions, the wave function must vanish for large values of $w$. This requirement is satisfied only if $s$ is real. Using this boundary condition, the solution to Eq. (1) can be written in three regions:

$$\begin{aligned} &H(w)=A_1e^{sw}, && w\leq -1\\ &H(w)=A_2e^{itw}+B_2e^{-itw}, && -1\leq w<+1\\ &H(w)=B_1e^{-sw}, && w\geq +1. \end{aligned} \tag{12}$$

For the logarithmic derivatives to be continuous at $w=-1$ and $w=+1$, the following relationship must apply:

$$\begin{aligned} &s=it\frac{A_2e^{-it}-B_2e^{+it}}{A_2e^{-it}+B_2e^{+it}}, \quad w=-1\\ &s=-it\frac{A_2e^{+it}-B_2e^{-it}}{A_2e^{+it}+B_2e^{-it}}, \quad w=+1. \end{aligned} \tag{13}$$

Equations (13) can be put in the form of two homogeneous equations in $A_2$ and $B_2$. For a nontrivial solution of these equations to exist, the following condition must be satisfied:

$$0=e^{-2it}(s-it)^2-e^{2it}(s+it)^2. \tag{14}$$

For this equation to have a solution with $s$ real and positive, $t$ must be real. Depending on the value of $t$ there are two different solutions to Eq. (14) for $s(t)$:

$$\begin{aligned} &s=t\tan(t), \quad n\pi<t<(n+\tfrac{1}{2})\pi \quad n=0,1,2\cdots\\ &s=-t\operatorname{ctn}(t),\\ &\qquad (n+\tfrac{1}{2})\pi<t<(n+1)\pi \quad n=0,1,2\cdots. \end{aligned} \tag{15}$$

These two solutions can be combined in a single relationship:

$$\begin{aligned} &t=\theta+\tfrac{1}{2}n\pi, \quad s=(\theta+\tfrac{1}{2}n\pi)\tan(\theta)\\ &0\leq\theta\leq\tfrac{1}{2}\pi, \quad n=0,1,2\cdots. \end{aligned} \tag{16}$$

A set of parametric equations, which specify $\lambda$ as a

function of parameters of the well, are obtained by combining Eqs. (9), (11), and (16):

$$V=\gamma_u^2(\theta_1+n_1\tfrac{1}{2}\pi)^2(1+\tan^2\theta_1),$$
$$0\leq\theta_1\leq\tfrac{1}{2}\pi \quad n_1=0, 1, 2\cdots$$
$$E_u=\tfrac{1}{2}\gamma_u^2(\theta_1+n_1\tfrac{1}{2}\pi)^2(1-\tan^2\theta_1),$$
$$V=\gamma_v^2(\theta_2+n_2\tfrac{1}{2}\pi)^2(1+\tan^2\theta_2), \qquad (17)$$
$$0<\theta_2<\tfrac{1}{2}\pi \quad n_2=0, 1, 2\cdots$$
$$E_v=\tfrac{1}{2}\gamma_v^2(\theta_2+n_2\tfrac{1}{2}\pi)^2(1-\tan^2\theta_2),$$
$$\lambda=E_u+E_v.$$

Equations (17) can be solved for the maximum well dimensions $(d_1,d_2)$ which give negative values of $\lambda$, i.e., dislocation bands as a function of well depth $V$. The resulting parametric relationship between $d_1$ and $d_2$, with $V$ as the parameter, gives the locus of $\lambda=0$. In Fig. 2 this solution is shown for the lowest value of $\lambda$ ($n_1=0$, $n_2=0$), at several values of $V$. This figure shows that at the dimensions assumed for the potential well (6 by 8 Å), the well must be almost 2.5 eV deep for even one dislocation band to exist. For more than one band to exist, the well must be much deeper. An energy of 2.5 eV is close to the band gap in CdS, and corresponds to the minimum energy difference between a bound and a free electron in a perfect lattice. This is a reasonable upper limit for the potential associated with a broken bond. Therefore CdS should contain no more than one dislocation band.

A second way to represent the solution to Eqs. (17) is to assume a value for the well depth, and then plot

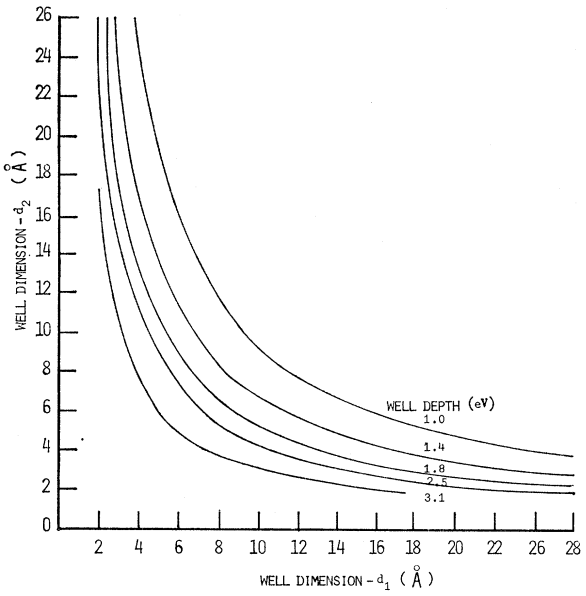


FIG. 2. Parametric curves showing the minimum well dimensions for which a dislocation band will exist. The parameter indicated on these curves is the depth of the pseudo-square-well. In making these calculations a value of 0.2 was assumed for the effective mass of the electron.

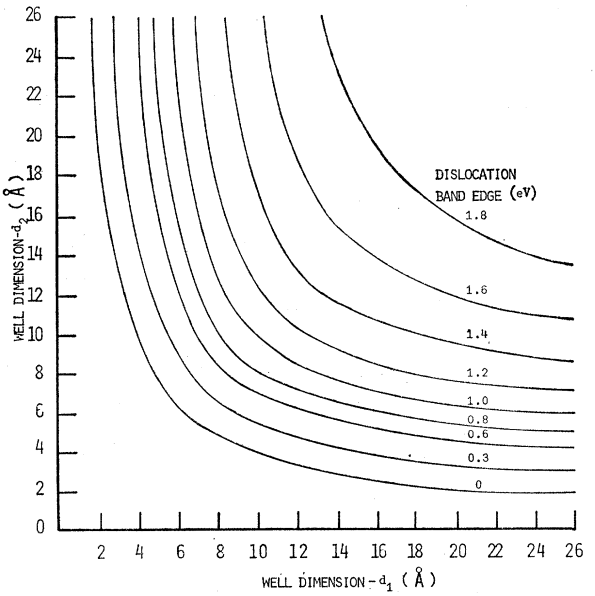


FIG. 3. Parametric curves showing the well dimensions which give identical values for the dislocation band edge in a pseudo-square-well which is 2.5 eV deep. The parameter indicated on these curves is the value of the dislocation band edge. In making these calculations a value of 0.2 was assumed for the effective mass of the electron.

the parametric relationship between the widths of the well $(d_1,d_2)$ using the band edge $\lambda$ as a parameter. In Fig. 3 a well depth of 2.5 eV is assumed, and the well sizes which give various binding energies between 0 and 1.8 eV are plotted. In the calculations for Figs. 2 and 3, a value of $0.2m_e$ was used for the effective mass; this is an average of the experimental values reported for the effective mass of the electron in the conduction band of CdS.[13–17]

## 4. OCCUPATION OF DISLOCATION BANDS

To find the occupation of a dislocation band, it is assumed that there is little interaction among the captured electrons, and their distribution is given by a Fermi function

$$f_k(W_T)=\left[1+\exp\frac{W_T-E_F}{k_bT}\right]^{-1}, \qquad (18)$$

where

$$W_T=\lambda+E(0,0,\hbar k)-V_a, \qquad (19)$$

and both $W_T$ and $E_F$ are measured (positive up) from the conduction-band edge.

[13] W. W. Piper and R. E. Halsted, in *Proceedings of the International Conference on Semiconductor Physics, 1960* (Czechoslovakian Academy of Sciences, Prague, 1961), p. 1048.
[14] W. W. Piper and D. T. F. Marple, J. Appl. Phys. **32**, 2237 (1961).
[15] M. Cardona, J. Chem. Phys. Solids **24**, 1543 (1963).
[16] J. J. Hopfield and D. G. Thomas, Phys. Rev. **122**, 35 (1961).
[17] F. A. Kroger, H. J. Vink, and J. Volger, Philips Res. Rept. **10**, 39 (1955).

To find the average number of captured electrons per unit dislocation length ($n_D$), Eq. (18) must be summed over all allowed values of $k$. As usual, this summation is replaced by the following integration:

$$n_D=\frac{2}{\pi}\int_0^\infty f_k(W_T)dk, \tag{20}$$

where $E(0,0,\hbar k)$ is assumed to be a symmetric function of $k$. Equation (20) can be integrated by parts; the integrated part vanishes with the result

$$n_D=\frac{2}{\pi}\int_0^\infty k df_k(W_T). \tag{21}$$

To solve Eq. (21) the usual free-electron relationship is assumed:

$$E(0,0,\hbar k)=\hbar^2k^2/2m, \tag{22}$$

where $m$ is the effective mass for motion in the $z$ direction. For convenience we make the following definitions:

$$f(z)=(1+e^z)^{-1},$$
$$z=\frac{W_T-E_F}{k_bT}=\frac{1}{k_bT}[\lambda-V_q-E_F+\hbar^2k^2/2m], \tag{23}$$
$$B=-\frac{1}{k_bT}(\lambda-V_q-E_F).$$

The function $f(z)$ is a conventional Fermi function in which the energy $z$ is translated to the origin, and the argument $z$ is expressed in units of $k_bT$. The only case considered here is that of the Fermi energy within the dislocation band, i.e., that of positive $B$. Combine Eqs. (21) and (23):

$$n_D=\frac{2}{\pi}\left[\frac{2m}{\hbar^2}k_bT\right]^{1/2}\int_{-B}^\infty (z+B)^{1/2}\left(-\frac{df}{dz}\right)dz. \tag{24}$$

Since the derivative of $f(z)$ looks like a $\delta$ function, the value of this integral is determined near the origin. Thus the integral can be approximated by expanding $(z+B)^{1/2}$ in a power series about the origin, and replacing the lower limit of integration by $-\infty$. The integrals in the resulting series can be evaluated explicitly:

$$n_D=\frac{2}{\pi}\left[\frac{2m}{\hbar^2}k_bTB\right]^{1/2}\left[1-\frac{\pi^2}{25}B^{-2}+\cdots\right]. \tag{25}$$

If the Fermi energy is more than a few $k_bT$ above the band edge, the dislocation occupation can be approximated by the first term in Eq. (25). Combining this approximation with the definition of $B$ [Eq. (23)] gives

$$n_D=\frac{2}{\pi}\left[\frac{2m}{\hbar^2}\right]^{1/2}(E_F+V_q-\lambda)^{1/2}. \tag{26}$$

Using Eq. (1) to eliminate $V_q$ in Eq. (26) gives

$$n_D=K[E_F-\lambda+\tfrac{1}{2}Cn_s-Cn_D]^{1/2},$$
$$K=\frac{2}{\pi}\left[\frac{2m}{\hbar^2}\right]^{1/2}. \tag{27}$$

Equation (27) establishes an implicit relationship between $n_D$ and $E_F$. This equation is analogous to the usual relationship between the occupation $n_j$ of a local energy level at $E_j$ and the Fermi energy:

$$n_j=N_j\left[1+\exp\frac{E_j-E_F}{k_bT}\right]^{-1}, \tag{28}$$

where $N_j$ is the density of these levels. In both Eqs. (27) and (28), the occupation ($n_D$ or $n_j$) is determined when the Fermi energy is specified.

## 5. FERMI ENERGY IN A CRYSTAL CONTAINING DEFECTS

In a crystal containing defects the Fermi energy is determined by the temperature and the number and type of defect levels present. An analytical relationship between $n_D$, $n_j$, and $E_F$ can be derived from the equation of charge neutrality, and from continuity equations for the local levels and the dislocation bands

$$n+\sum n_a=p+\sum p_d+N_Dp_D, \tag{29}$$
$$n_j+p_j=N_j, \tag{30}$$
$$n_D+p_D=n_s, \tag{31}$$

where $n_a$ represents electrons occupying acceptor sites, $p_d$ represents holes occupying donor sites, $N_D$ represents the density of dislocation lines, and $n_D$ and $p_D$ represent the electron and hole occupation of the dislocation bands.

By applying Eq. (30) to each of the donor levels, and then summing over all donor levels, $\sum p_d$ can be eliminated from Eq. (29):

$$-n-\sum n_a+p+\sum N_d-\sum n_d+p_DN_D=0, \tag{32}$$

where $\sum N_d$ represents the total number of donor levels in the crystal. The terms $\sum n_a+\sum n_d$, which represent the number of electrons occupying all of the local levels, can be rewritten as

$$\sum n_a+\sum n_d=n_j+\sum n_B+\sum n_A, \tag{33}$$

where $n_j$ is the number of electrons occupying the level nearest the Fermi energy, $\sum n_B$ is the number of electrons occupying local levels below $E_j$ ($E_j$ is the energy of the $j$th level), and $\sum n_A$ is the number of electrons occupying levels above $E_j$. Combining Eqs. (31), (32), and (33), and using (30) to eliminate $\sum n_B$ yields

$$\sum N_B+n_j=\sum N_d+N_D(n_s-n_D)+M, \tag{34}$$

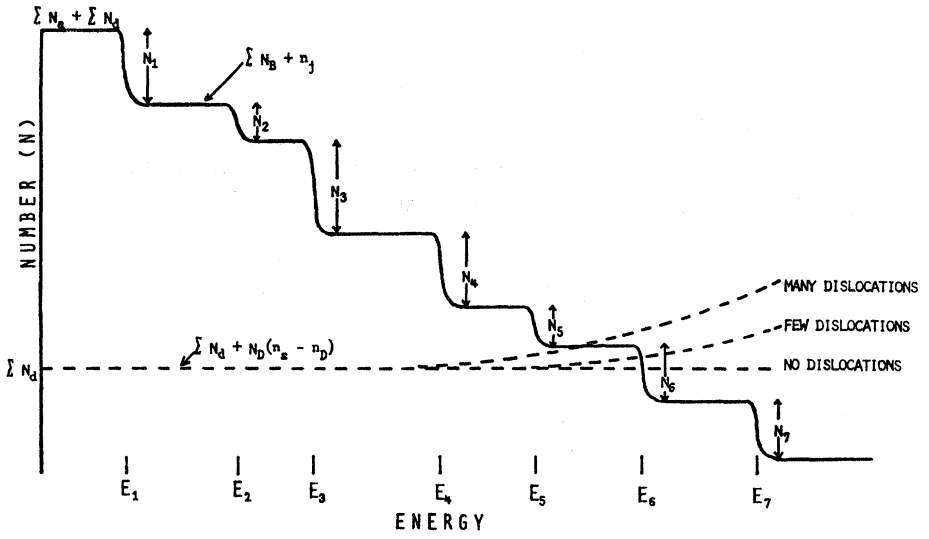


FIG. 4. Solution to $\sum N_B+n_j = \sum N_d+N_D(n_s-n_D)+M$ for hypothetical crystal.

where $\sum N_B$ is the total number of local levels lying below $E_F$, and $M$ is defined by

$$M=p+\sum p_B-n-\sum n_A. \tag{35}$$

$M$ is the difference between the number of holes in local levels below $E_j$ and the number of electrons in levels above $E_j$. Since $E_j$ is the local level nearest the Fermi energy, and because of the sharpness of the Fermi function, both of these quantities are small. Therefore $M$ is small.

An implicit equation for $E_F$ can be obtained by combining Eqs. (27), (28), and (34). To obtain the Fermi energy explicitly we plot the left- and right-hand sides of Eq. (34) independently, as a function of $E_F$, using Eqs. (27) and (28) to determine how $n_j$ and $n_D$ depend on $E_F$. The Fermi energy for the crystal is given by the intersection of these two curves. Because of the steplike nature of the Fermi function, the left-hand side of Eq. (34) is essentially constant between the local levels, and at $E_j$ it decreases by $N_j$ over an energy of a few $k_bT$. The right-hand side of Eq. (34) is dominated by the constant term $\sum N_d$; however, in a crystal containing dislocations, the term $n_D$ [Eq. (27)] gives it curvature.

In Fig. 4, solid and dashed curves represent the left- and right-hand sides of Eq. (34) which are plotted for a hypothetical crystal with various dislocation contents. In the dislocation-free case the solid and dashed curves are parallel everywhere except very near the local levels. Thus the intersection must occur very near one of these levels. However, in the crystal with dislocations, the two curves are no longer parallel and intersections can occur between the local levels. For example, in Fig. 4, the Fermi energy is near $E_6$ in the dislocation-free case, as well as in the case of few dislocations, but with many dislocations the Fermi energy is between $E_5$ and $E_6$.

With these graphical solutions in mind, appropriate approximations can be made to obtain an analytic expression for $E_F$. First, consider the dislocation-free case. Letting $N_D=0$, combine Eqs. (34) and (28), and solve for $E_F$:

$$E_F=E_j-k_bT\ln[N_j/(\sum N_d-\sum N_B+M)-1]. \tag{36}$$

Equation (36) can be used to determine the activation energy which governs the temperature dependence of the electrical conductivity. In the case of CdS, which is an $n$-type, wide-band-gap semiconductor, the electrical conductivity is given by

$$C=nq\mu=N_cq\mu\exp[E_F/k_bT], \tag{37}$$

where $q$ is the charge on an electron and $\mu$ is the mobility and the zero of energy is defined at the conduction-band edge. Combine (36) and (37):

$$\ln C=(1/k_bT)E_j+\ln N_cq\mu -\ln[N_j/(\sum N_d-\sum N_B+M)-1]. \tag{38}$$

By definition,[18] $N_c$ is proportional to $T^{+3/2}$ and experimentally,[19] between 80 and 700°K, the mobility in CdS is proportional to $T^{-3/2}$, hence $\mu N_c$ is temperature-independent. In addition, as mentioned earlier, $M$ is small, so its temperature dependence can be neglected in the last term. Therefore, in a dislocation-free crystal, the slope of a plot of $\ln C$ versus $1/k_bT$, i.e., the "activation energy," will be $E_j$.

For a crystal containing dislocations, the case in which the Fermi level is near a local level must be distinguished from the case where it is between two local levels. Figure 4 shows that in the former case the

[18] R. H. Bube, *Photoconductivity of Solids* (John Wiley & Sons, Inc., New York, 1960).
[19] W. E. Spear and J. Mort, Proc. Phys. Soc. (London) **81**, 130 (1963).

exact value of $E_F$ is determined by the variation of $n_j$ with energy, and $n_D$ can be treated as if the intersection were at the local level. In this case $E_F$ is given by

$$E_F=E_j-k_bT\ln\{N_j/[\sum N_d-\sum N_B+M+N_Dn_s-N_Dn_D(E_j)]-1\}. \quad (39)$$

By comparing this result to Eq. (36), we can see that the activation energy is again $E_j$.

When the Fermi energy falls between two of the local levels, $n_j$ is either 0 or $N_j$, and it is not a strong function of energy. In this case $E_F$ can be found by combining Eqs. (34) and (27):

$$E_F=\lambda+\frac{1}{K^2N_D^2}[\Sigma N_d+N_Dn_s+M'-\Sigma N_B]^2 + \frac{C}{N_D}[\Sigma N_d+\tfrac{1}{2}N_Dn_s+M'-\Sigma N_B], \quad (40)$$

where $M'$ is defined by

$$M'=M-n_j(E), \quad |E-E_j|>k_bT. \quad (41)$$

In this case the activation energy is equal to $E_F$ and it will be between two of the local levels.

## 6. EXPERIMENT TO TEST THE PREDICTIONS

Light with energy less than the band gap changes the distribution of charge carriers by exciting electrons to levels above $E_F$ and holes to levels below $E_F$. This can be described in terms of a change in the value of $M$ with light intensity. According to the quasi-Fermi-level concept[20] only recombination centers are sufficiently far from either band to experience a significant departure from the thermal equilibrium distribution of charge carriers. Therefore the charges that occur in $M$ when the crystal is illuminated are primarily caused by changes in the occupation of the recombination centers. CdS contains recombination centers (sensitizing centers) which have the property that their occupation by holes increases with light intensity.[20] It is likely that holes accumulating in the sensitizing centers will be the dominant contribution to $M$. Therefore, in CdS we would expect $M$ to increase with light intensity, and since the occupation of the sensitizing levels is not strongly affected by changes in Fermi energy or temperature,[20] $M$ should not depend on $E_F$ or $T$.

$M$ appears on the right-hand side of Eq. (34), so in Fig. 4 the dashed curves move rigidly upwards as the intensity of the light is increased. The amount of this displacement is related to the number of holes trapped by the sensitizing levels. In dislocation-free crystals, the solid and dashed curves are parallel everywhere except near the local energy levels. Thus as the dashed curve moves up, the intersection which determines the Fermi energy must move discontinuously between the local levels. On the other hand, in crystals with dislocations, these two curves are not parallel and as the dashed curve moves up, their intersection can move continuously between the local levels. However, between these transition regions, there will be ranges of light intensity over which the Fermi energy is very near one of the local levels.

We conclude that in dislocation-free crystals, the activation energy, when measured as a function of light intensity, will change discontinuously between energies corresponding to the local levels. In a crystal containing dislocations, the activation energy will have plateaus at energies corresponding to the local levels, and there will be continuous transition regions between these plateaus.

## 7. EXPERIMENTAL PROCEDURE

In order to standardize the defect content as much as possible, all samples studied were cut from one large, single crystal of CdS. This crystal was not intentionally doped, and appeared clear and of uniform color. This crystal was cut into rectangular parallelepipeds, each measuring approximately $2\times2\times5$ mm$^3$. These samples are oriented so that the $\langle1\bar{1}00\rangle$ direction is along their length, and the $\langle11\bar{2}0\rangle$ and $\langle0001\rangle$ directions are along the diagonals of their ends. Prior to deformation, the conductivity of the samples fell in the range $3.5\times10^{-10}$ to $7.4\times10^{-10}$ $(\Omega\text{ cm})^{-1}$ at 119°C.

The samples were deformed to strains of between 1 and 22% by the application, at 400°C, of a static longitudinal stress of between 1.0 and 3.0 kg/mm$^2$. The crystals were heated under these stresses, in a helium atmosphere, to 580°C. Although the change in dislocation density with plastic strain in CdS is not known, the relation is expected to be monotonic for the strains used in these experiments. During these deformations, a second sample (reference crystal) is placed close enough to the crystal being deformed to be at the same temperature.

The optical experiment proposed earlier was accomplished by measuring the conductivity of the crystals as a function of temperature under different amounts of illumination. The crystals were illuminated with light from a 500-W incandescent lamp (G.E. type DHJ). An interference filter with a peak wavelength of 7000 Å and a bandwidth of 280 Å was used as a monochromator. Neutral density filters were used to control the light intensity.

By comparing the absorption of a slab of CdS and the absorption of various neutral density filters, it was determined that the CdS had an absorption length (distance required to reduce the intensity by a factor of $e^{-1}$) of 1.94 mm at the wavelength used in these experiments. Since the thickness of the samples tested was 1.8 to 1.9 mm, it follows that the light is absorbed throughout the samples, hence we observe bulk effects and not surface effects.

[20] R. H. Bube, J. Phys. Chem. Solids **1**, 234 (1957).

The illumination was varied over a flux range of $10^{11}$ to $10^{12}$ photons/cm$^2$ sec. At the lower intensity limit the activation energy was generally unchanged from its dark value, and at the upper limit, the amount of optical excitation into the conduction band became so large that it was impossible to determine accurately the activation energy of the thermal process.

Ohmic, soldered indium contacts were used on all samples. To reduce the possibility of contact error, all measurements were made with $30\pm0.3$ V applied to the sample. The sample conductance was measured in a series circuit which consisted of a regulated 30-V dc power supply, a Keithley Model 610A Electrometer, and the sample. The thermal activation energy was determined from the temperature dependence of the sample's conductance, during a heat-cool cycle, between room temperature and 127°C.

For measurements made in the dark, a plot of $\ln C$ versus $1/T$ was found to be linear over the entire temperature range. However, the determination of the activation energy from measurements made with illumination is complicated by optically excited electrons. This is because the relationship between $E_F$ and $C$, given by Eq. (37), applies only to thermally excited conductance; if the optically excited conductance is included then Eq. (37) defines the quasi-Fermi-level.[20] Thus in illuminated crystals these two contributions to the conductivity must be separated.

Figure 5 shows the data for a crystal under illumination. The observed relationship between conductance and $1/T$ (solid curve) has a minimum which arises from the difference between the temperature dependence of the conductance due to the optically and thermally excited electrons. At high temperatures the thermally excited electrons dominate, and the conductance increases exponentially with increasing temperature (thermal activation). At lower temperatures, optically excited electrons dominate, and the conductivity decreases with increasing temperature (thermal quenching).

These two contributions to the conductivity are separated by a self-consistent analysis. To do this a line is drawn which approximately fits the thermal-quenching portion of the data. Values of the conductivity on this line are subtracted from all data in order to estimate points on the thermal activation curve. A line is then drawn through these points and values of conductivity from this line are subtracted from the original data to obtain a better estimate of the thermal quenching curve. After several (usually three) repetitions of this process, the original data can be separated into two straight line segments. The dashed lines in Fig. 5 represent the results of this decomposition technique. The activation energies obtained in this manner are accurate to $\pm0.02$ eV.

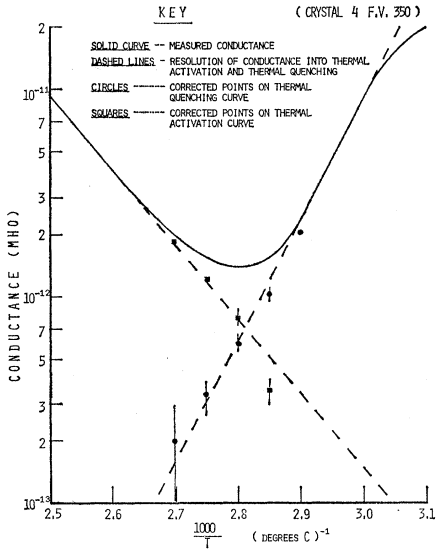


FIG. 5. Example demonstrating how the measured conductivity data are separated into an optical and a thermal contribution.

## 8. RESULTS

The experiments discussed above have been conducted on nine samples (five deformed, four reference). In Figs. 6–9 the thermal activation energy for these nine samples is plotted as a function of relative light intensity. An intensity of unity corresponds to a flux of $10^{11}$ photons/cm$^2$ sec. The activation energy plotted in these figures is the average of two values: one calculated from data taken on heating and the other from data taken on cooling. When these two values differ by more than the experimental uncertainty of 0.02 eV, error brackets are included.

The results shown in Figs. 6–9 have the form predicted. Both the reference crystal and the deformed crystal show two ranges (plateaus) where the activation energy is essentially independent of light intensity. The "transition region" between these two "plateaus" is sharp in the case of the reference crystals and broad in the case of the deformed crystals. The plateaus

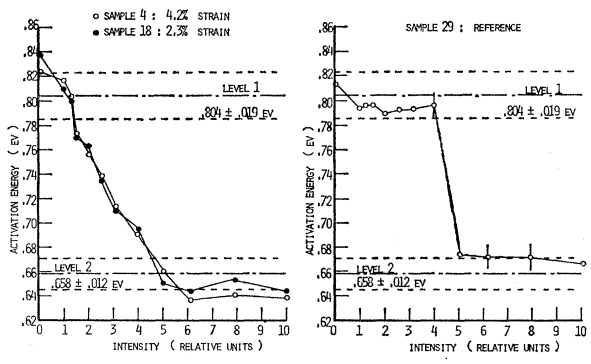


FIG. 6. Activation energy as a function of the relative intensity of the 7000 Å light.

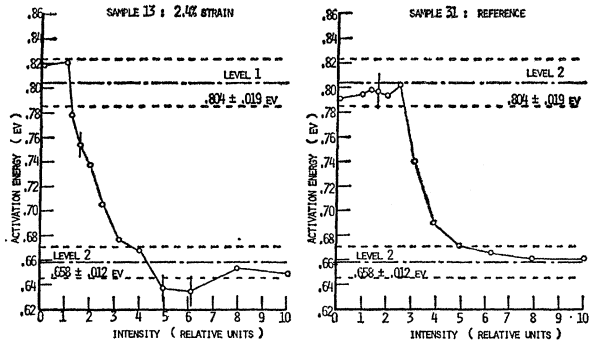


FIG. 7. Activation energy as a function of the relative intensity of the 7000 Å light.

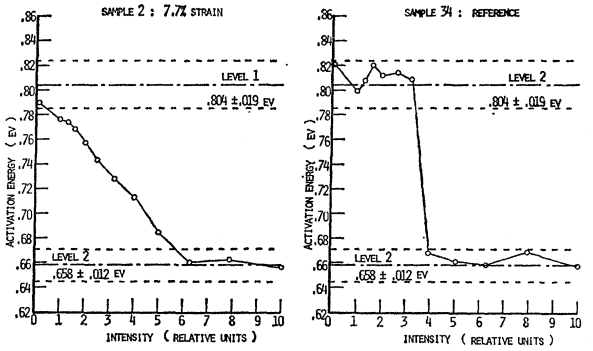


FIG. 8. Activation energy as a function of the relative intensity of the 7000 Å light.

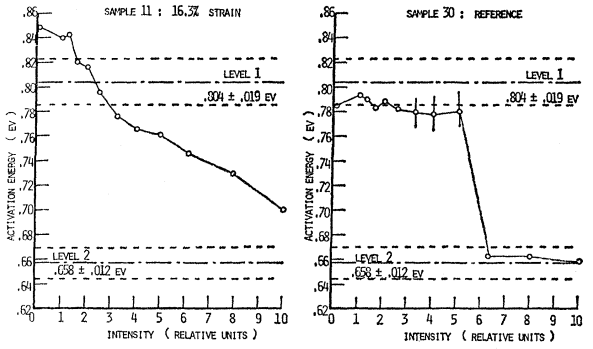


FIG. 9. Activation energy as a function of the relative intensity of the 7000 Å light.

correspond to light intensity ranges over which the activation energy is equal to the energy of a local level, and the transition region corresponds to intensity ranges over which the activation energy is between two local levels. Since these samples were all cut from the same single crystal they are expected to contain the same local levels, and the activation energy plateaus should occur at the same energy in all nine samples. The average value, for all samples, of the points on the upper plateau is 0.804±0.019 eV and on the lower

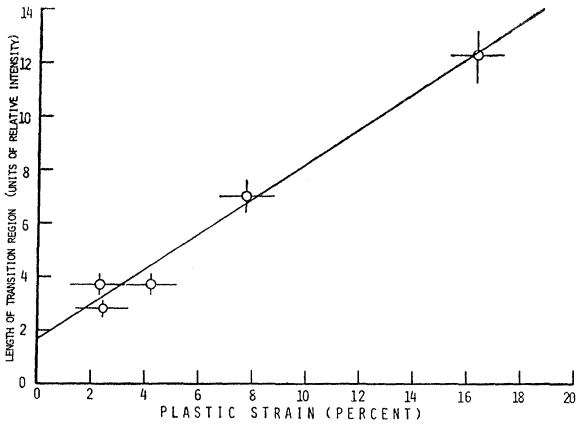


FIG. 10. Relationship between plastic strain and the observed range of light intensities over which the thermal activation energy is between the plateaus corresponding to levels one and two.

plateau it is 0.658±0.012 eV. The error indicated represents one standard deviation, and is slightly less than the measurement uncertainty (0.02 eV). These plateaus, therefore, constitute evidence for two different discrete levels in CdS.

Several features of Figs. 6–9 warrant mention:

*Figure 6.* Samples 4 and 18 were deformed together, under the same stress, and the results obtained on them are nearly identical. Thus they apparently have similar dislocation content, due to similar strain hardening.

*Figure 7.* The reference crystal has one measured point for activation energy within the transition region. The fact that no such points were detected for the other reference crystals may be evidence that they contained fewer dislocations.

*Figure 9.* The activation energy of the deformed crystal is above the lower plateau at the brightest light tested. This indicates that this sample contains a very high dislocation density, and the maximum light intensity used was not sufficient to reach the lower plateau.

From Fig. 4 we can see that the range of the parameter $M$ over which the activation energy is between two local levels increases with dislocation content. Since $M$ increases monotonically with light intensity, and the dislocation content increases monotonically with plastic strain, the range of intensities over which the activation energy is between the two local levels should be a monotonically increasing function of plastic strain. Figure 10 shows a plot of the observed length of the transition region as a function of the amount of plastic strain. The relationship between these variables is linear within the range tested.

## 9. DISCUSSION AND CONCLUSIONS

A quantum-mechanical treatment of the electronic levels associated with dislocations, and a statistical treatment of dislocation occupation were carried out. It is concluded that bands of energy states are as-

sociated with edge dislocations and the occupation of these states can be predicted from a knowledge of the Fermi energy. By combining this derived dislocation occupation function with a general description of a wide-band-gap semiconductor containing many deep levels and a donor dislocation band, we were able to predict that by measuring, in illuminated crystals, the thermal activation energy associated with the electrical conductivity, as a function of light intensity, energy plateaus will be detected in all crystals. In crystals with a low dislocation density, these plateaus will be connected by sharp transition regions, and in deformed crystals, these plateaus will be connected by broad transition regions.

The experimental data reported in the preceding section agree with this prediction. Indeed, in the reference crystals the transition extends over a change in illumination intensity of $1.7\times10^{11}$ photons/cm$^2$ sec or less, whereas in the deformed samples, as seen in Fig. 10, the range is between $2.8\times10^{11}$ and $13\times10^{11}$ photons/cm$^2$ sec. These results are consistent with the band formulation of electron energy states associated with dislocations in CdS. Further, we can conclude that in the crystals investigated, the Fermi energy falls within a donor dislocation band.

Since the Fermi energy for the samples tested was about 0.8 eV below the conduction band, and it fell within the dislocation band, we can conclude that the dislocation band edge must be more than 0.8 eV below the conduction-band edge. From the solution of the "square-well" dislocation potential (Fig. 3), we can see that for the dislocation band edge to be more than 0.8 eV below the conduction-band edge, a well 2.5 eV deep must extend over an area of 10 by 10 Å or more. These dimensions are to be compared with values of 6 by 8 Å which were estimated from geometric considerations. In light of the approximations made in this theory, this is considered to be reasonable agreement.

In addition to dislocations, plastic deformation may introdude point defects into the solid. According to the analysis of Sec. 5 these point defects may introduce new plateaus in the activation energy versus light intensity relationship, but they cannot cause a broad transition region. Experimentally, we observed broad transition regions in all deformed crystals, but we found no evidence for new local levels. Therefore, we conclude that in these experiments we are seeing effects due to the energy states associated with dislocations, rather than effects due to point defects introduced during deformation.

We conclude that dislocations in CdS have donor bands associated with them and the donor band edge lies more than 0.8 eV below the conduction band. Further we have shown that it is possible to use local levels (in this case at 0.80 and 0.66 eV) as a probe of the dislocation band, and we have verified that it is possible to observe continuous changes in the location of the Fermi energy as the occupation of the dislocation band is increased by optical excitation. Finally, we note that the results shown in Fig. 10 indicate that the range of light intensity over which the activation energy is between two local levels is proportional to plastic strain.